

Table 1. Computational conditions.

$L_x \times L_y \times L_z$	$731.4\delta \times 2\delta \times 365.7\delta$
$N_x \times N_y \times N_z$	$4096 \times 64 \times 2048$
$\Delta x^+, \Delta z^+$	10
$\Delta y_{\min}^+ - \Delta y_{\max}^+$	0.295–3.54
Δt^+	0.0224

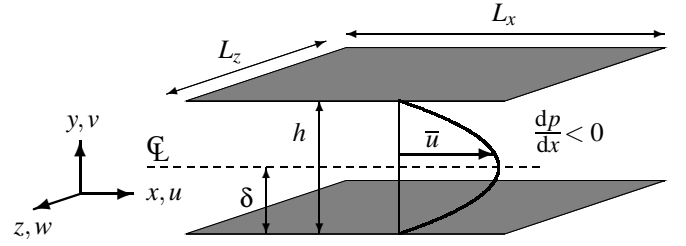


Figure 1. Configuration of channel flow.

was triggered by initial random disturbances. They also used a turbulent spot as an initial condition and observed that the spot developed into turbulent stripe for some range of the Reynolds number.

It can be anticipated that a spot in the plane Poiseuille flow at a transitional Reynolds number should develop into the turbulent stripes. We have performed a large-scale DNS of growth of a turbulent spot in the channel flow and examined its growth process.

NUMERICAL PROCEDURE

The mean flow is driven by a uniform pressure gradient, as shown in Fig. 1. The periodic boundary condition is imposed in the horizontal directions and the non-slip condition is applied on the walls. The coordinates and flow variables are normalized by u_τ , v and δ . The fundamental equations are the continuity and the Navier-Stokes equations:

$$\frac{\partial u_i}{\partial x_i} = 0, \quad (1)$$

$$\frac{\partial u_i^+}{\partial t^*} + u_j^+ \frac{\partial u_i^+}{\partial x_j^*} = -\frac{\partial p^+}{\partial x_i^*} + \frac{1}{Re_\tau} \frac{\partial^2 u_i^+}{\partial x_j^{*2}} + \delta_{1i}, \quad (2)$$

where δ_{1i} corresponds to the mean pressure gradient and quantities with the superscript of * indicate those normalized by the outer variables, e.g., $x^* = x/\delta$, and the superscript of + indicates the normalization by the inner variables, e.g., $u^+ = u/u_\tau$. For the spatial discretization, the finite difference method is adopted. The numerical scheme with the 4th-order accuracy is employed in the streamwise and spanwise directions, while the one with the 2nd-order is applied in the wall-normal direction. Time advancement is executed by a semi-implicit scheme: the 2nd-order Crank-Nicolson method for the viscous term in the wall-normal direction and the 2nd-order Adams-Bashforth method for the other terms. Uniform grid mesh is used in the horizontal directions, and non-uniform mesh in the wall-normal direction. The

DNS has been made for $Re_\tau = 56$ with a large computational box size to allow the spot to develop into the turbulent stripe. Other detail numerical conditions are summarized in Table 1.

A laminar flow field is used as the initial condition. The turbulent spot is triggered by a vortex pair, which has the following analytical form:

$$\left. \begin{aligned} \psi &= A (1 - y^2)^2 z e^{-x^2 - z^2} \\ u &= 0 \\ v &= \psi_z \\ w &= -\psi_y \end{aligned} \right\} \quad (3)$$

where A is an amplitude coefficient and chosen such that the maximum initial wall-normal velocity is the same as the magnitude of center-line streamwise velocity. This simple double vortices were adapted by Henningson et al. [6] as the initial disturbance. It has been known from experimental investigations of spots in various types of flows that the spot characteristics become essentially independent of the initial disturbance if its magnitude is strong enough to develop.

RESULTS AND DISCUSSION

Instantaneous velocity

Figure 2 shows contours of instantaneous distribution of wall-normal velocity in the (x, z) -plane at the channel center, presenting a temporal evolution of the turbulent spot. Although the vortex pair of the initial disturbance rapidly broke down, it gives rise to a turbulent spot with propagating downstream: see Fig. 2(a). In front of the spot, a disturbed but non-turbulent region (quasi-laminar region) can be found and the turbulent region appeared in the form of an arrowhead shape. Within the spot, turbulent eddies were preceded by oblique waves, as shown in an enlarged view of the figure. Additional oblique waves were also found at the rear spanwise tips of the spot. These findings are in consistent with those observed by Carlson et al. [5] and Henningson et al. [6].

The turbulent region splits in the spanwise direction and takes in the form of a V-shape, as given in Fig. 2(b). Carlson

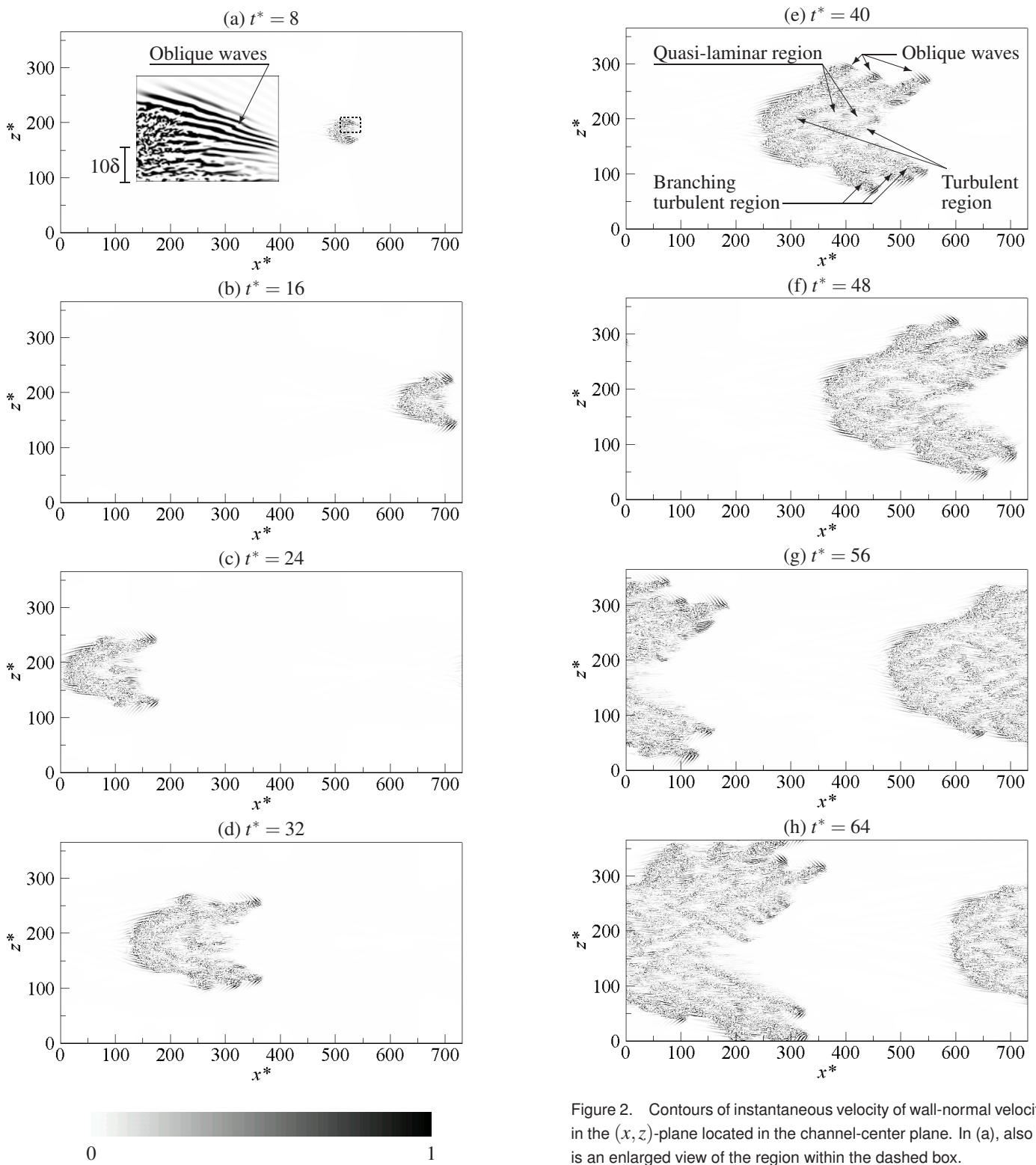


Figure 2. Contours of instantaneous velocity of wall-normal velocity (v^+) in the (x, z) -plane located in the channel-center plane. In (a), also shown is an enlarged view of the region within the dashed box.

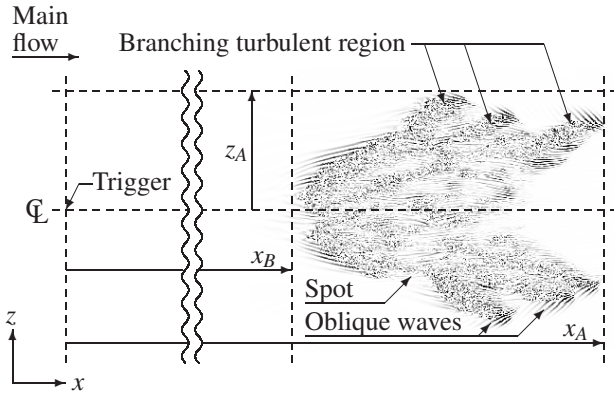


Figure 3. Turbulent spot nomenclature.

et al. [5] also observed the development of the splitting spot. The turbulent spot sustains oblique waves at the spanwise interface of the spot. At the center of the spot, turbulence propagates and a new turbulent region emerges, as given in Fig. 2(c). Quasi-laminar and turbulent regions coexisted in the turbulent spot (Fig. 2(d)), and each region became multiple V-shape. The streamwise wavelength λ_x and the spanwise wavelength λ_z of a pair of a quasi-laminar region and a turbulent region are estimated from the figures, and they are 50δ and 20δ , respectively. Tsukahara et al. [2, 3] observed that λ_x was 66δ and λ_z was 22δ in the fully-developed turbulent stripe. Hence the pattern wavelength inside the developing turbulent spot is smaller than that of the developed equilibrium state. However, λ_x in Fig. 2(e) is about 60δ , which is comparable to that of the fully-developed turbulent stripe. Then the turbulent region splits in the streamwise direction and another quasi-laminar region emerges between the turbulent bands. The inclination angle θ is an angle of a stripe structure to the streamwise direction. It can be seen from Fig. 2(d) and 2(e) that θ is 20° – 25° , which agrees well with that of the fully-developed turbulent stripe.

As growing to the size of $O(100\delta)$, the turbulent region started to branch at the edge of the spot, as shown in Figs. 2(d–f), and several branching turbulent regions developed parallel to each other obliquely to the streamwise direction with an angle of 20° – 25° : see also Fig. showing how the turbulent region develops and overhangs laminar region at the front and sides of the spot with accompanied by the several branches and oblique waves. This angle corresponds to θ in the fully-developed turbulent stripe, but the value of λ_x ranges from 50δ to 90δ . The branching turbulent region is wider than a turbulent band of the turbulent stripe. In Figs. 2(g) and 2(h), the branching turbulent regions split into quasi-laminar and turbulent regions. Their wavelengths of λ_x and λ_z are same with those of the fully developed turbulent stripe.

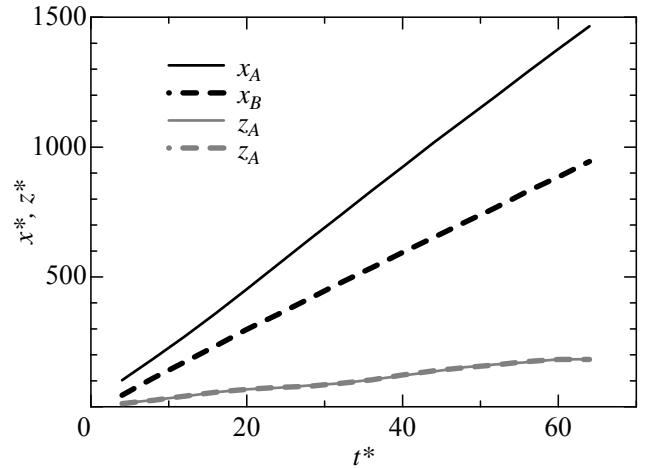


Figure 4. Temporal evolution of the spot. Point x_A is at the front interface, point x_B is at the rear interface, point z_A is at the top interface and point z_B is at the bottom interface of the spot.

Table 2. Propagation velocities of the spot.

Position of the spot	Propagation velocity	Propagation velocity By Henningson et al. [8]
$x_A / (tu_c / \delta)$	0.82	0.80
$x_B / (tu_c / \delta)$	0.53	0.54
$z_A / (tu_c / \delta)$	0.11	0.12

Spreading of disturbance

The positions of four points on the spot are shown as a function of time in Fig. 4. Point x_A represents the streamwise velocity position of the front interface of the spot, point x_B the rear interface, point z_A the spanwise top interface and point z_B the bottom interface: cf. Fig. . All points are seen to fall on straight lines, showing that their respective spot features propagate with constant speeds although turbulent region splits into quasi-laminar and turbulent regions and branches into three turbulent regions at the edge of the spot. The propagation velocities of the points z_A and z_B are found to be slightly decreased in $20 < t^* < 30$. During this period, the spot splits in the streamwise direction and quasi-laminar regions emerge between turbulent regions at $20 < t^* < 30$. Before that, it splits in the spanwise direction and takes V-shape. Turbulent region branches at the edge of the spot for $t^* > 30$. Therefore, the propagation (expanding) velocity in the spanwise direction decreases, while the spot split in the streamwise direction, but it keeps almost linear correlation with time.

In Table 2, the obtained propagation velocities are compared

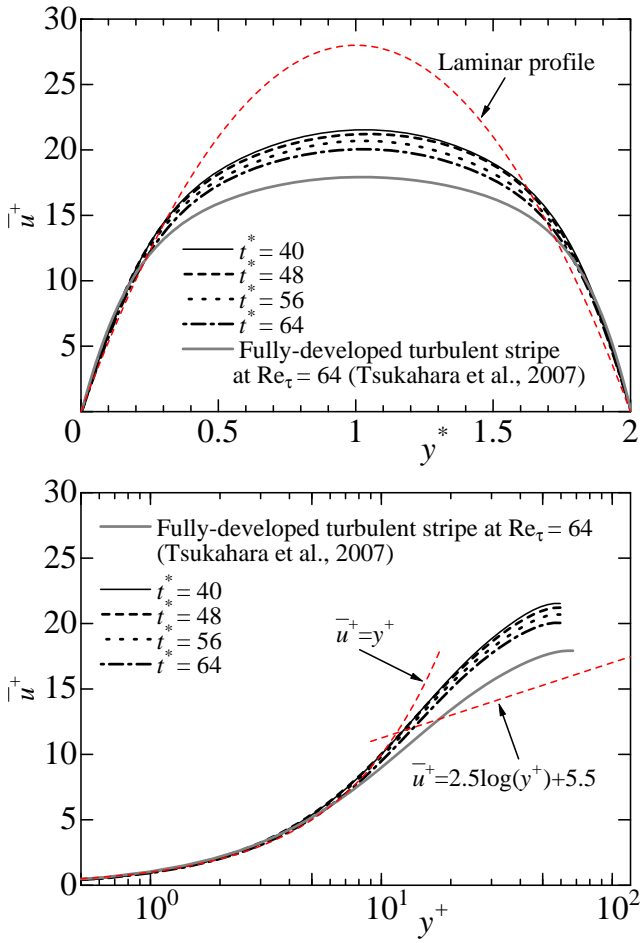


Figure 5. Mean velocity profile of the streamwise component inside the spot: (top) in outer units, (bottom) in wall units.

with those obtained by Henningson et al. [8], who also calculated them for $tu_c/\delta < 300$ at almost the same Reynolds number as our study but their calculation time was much less than the present one ($tu_c/\delta < 3500$). Here, u_c denotes the mean velocity at the channel center. The present results are in good agreement with the results of Henningson et al. [8] and found to remain nearly unchanged even as the shape of the spot changed dramatically from the arrowhead shape into the multiple V-shape.

Development of mean velocity profile

Figure 5 shows the vertical profiles of the dimensionless mean velocities. Here, an averaged statistic is denoted by a overline of $(\bar{\quad})$, which means the spatial averaging in the horizontal directions. We obtained the mean value in a finite area of $50\delta \times 50\delta$ inside the spot. The mean velocities are obtained for $40 < t^* < 64$ because the localized turbulent regions were observed to be larger than the size of $50\delta \times 50\delta$ at least for $t^* > 40$.

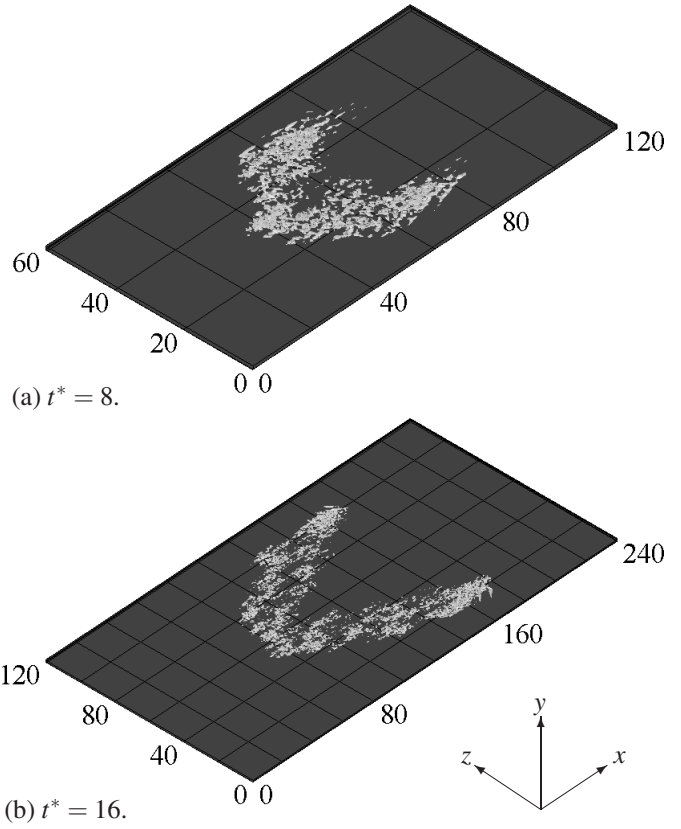


Figure 6. Iso-surfaces of second invariant of deformation tensor ($II^+ = u_{i,j}u_{j,i} \leq -0.025$), which equivalent to the vortical position. The direction of the mean flow is from bottom-left to top-right. The visualized volume is the lower half of the computational box.

As shown in Fig. 5, the mean streamwise velocity is faster than that of the fully-developed turbulent stripe. It can also be seen that the mean velocity slightly changes with time. Therefore, the mean velocity in the spot shows disagreement with that of the fully-developed turbulent stripe.

Vortex structure

Figure 6 shows the second invariant of deformation tensor:

$$II = \frac{\partial u_i^+}{\partial x_j^*} \frac{\partial u_j^+}{\partial x_i^*} \quad (4)$$

at (a) $t^* = 8$ and (b) 16. It can be easily found that vortex cluster takes a V-shape, not an arrowhead shape. No vortex can be seen in the downstream of the spot. Elongated vortices at the wing-tip regions are found, as shown later. In Fig. 6(b), the vortex cluster takes V-shape and no vortex can be seen in the downstream

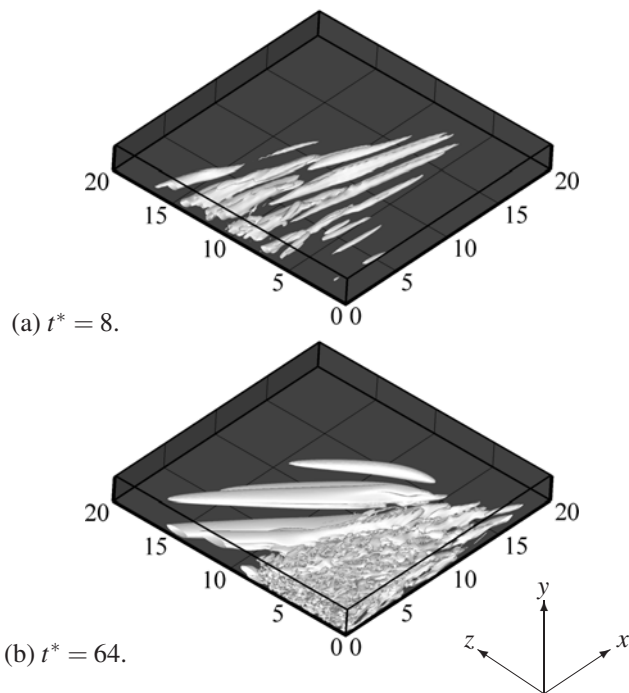


Figure 7. Vortical structures around the wing tip regions ($II^+ = u_{i,j}u_{j,i} \leq -0.5$). The direction of the mean flow is from top-left to bottom-right.

as similar to Fig. 6(a). There exist more vortices at the wing tip region than the other regions. It is also observed that several vortex clusters gives rise to branching turbulent regions and sparse regions among them.

Figure 7 presents vortical structures with emphasis on the wing tip region. The visualized volume is of $20\delta \times 2\delta \times 20\delta$. This alignment of vortices induces the oblique waves and make its wavelength to be about twice of the channel height as reported by Alavyoon et al. [9]. The vortices observed in Fig. 7(a) are inclined at angle of about 30° with respect to the streamwise direction, while most of vortices in Fig. 7(b) have angle of about 45° . Therefore, it can be said that the developed turbulent spot should have oblique waves but its structure is not identical to that of a well-known arrowhead-shape spot.

CONCLUSIONS

In the present study, we performed DNS of the turbulent spot developing into the turbulent stripes in a transitional channel flow at $Re_\tau = 56$ and investigated the characteristics of the flow.

We observed that, in a first stage, a vortex pair taken as the initial disturbance broke down and developed into a turbulent spot as it propagated downstream. The spot split in the spanwise direction and became V-shape, while it continuously grew by in-

creasing in length in the streamwise direction. Several branching turbulent regions and quasi-laminar region among them were observed to coexist in the turbulent spot and each region became in the form of multiple V-shape. Localized turbulent regions in the spot seemed to be elongated in oblique directions against the mean flow at an angle of about 30° , and we found six similar branches in the developing spot.

ACKNOWLEDGMENT

The present computations were performed with the use of the supercomputing resources at Cyber Science Center of Tohoku University. This work has been supported by KAKENHI (#20860070) and (#22760136).

REFERENCES

- [1] Tsukahara, T., Seki, Y., Kawamura, H., and Tochio, D., 2005. "DNS of turbulent channel flow at very low Reynolds numbers". In Proceedings Fourth International Symposium on Turbulence and Shear Flow Phenomena, J. A. C. H. *et al.*, ed., pp. 935–940.
- [2] Tsukahara, T., Seki, Y., Kawamura, H., and Tochio, D., 2007. "Turbulent heat transfer in a channel flow at transitional Reynolds numbers". In Proceedings of the First Asian Symposium on Computational Heat Transfer and Fluid Flow, p. 62.
- [3] Tsukahara, T., Kawaguchi, Y., Kawamura, H., Tillmark, N., and n, P. A., 2009. "Turbulence stripe in transitional channel flow with/without system rotation". In *Proceedings of the Seventh IUTAM Symposium on Laminar-Turbulent Transition*, P. Schlatter and D. Henningson, eds., Vol. 18 of *IUTAM Bookseries*. Springer, pp. 421–426.
- [4] Hashimoto, S., Hasobe, A., Tsukahara, T., Kawaguchi, Y., and Kawamura, H., 2009. "Experimental study on turbulent-stripe structure in transitional channel flow". In Proceedings of the Sixth International Symposium on Turbulence, Heat and Mass Transfer, pp. 193–196.
- [5] Carlson, D. R., Widnall, S. E., and Peters, M. F., 1982. "A flow-visualization study of transition in plane Poiseuille flow". *J. Fluid Mech.*, **121**, pp. 487–505.
- [6] Henningson, D. S., and Kim, J., 1991. "On turbulent spots in plane Poiseuille flow". *J. Fluid Mech.*, **228**, pp. 183–205.
- [7] Duguet, Y., Schlatter, P., and Henningson, D. S., 2010. "Formation of turbulent patterns near the onset of transition in plane Couette flow". *J. Fluid Mech.*
- [8] Henningson, D., Spalart, P., and Kim, J., 1987. "Numerical simulations of turbulent spots in plane Poiseuille and boundary-layer flow". *Phys. Fluids*, **30**, pp. 2914–2917.
- [9] Alavyoon, F., Henningson, D. S., and Alfredsson, P. H., 1986. "Turbulent spots in plane Poiseuille flow-flow visualization". *Phys. Fluids*, **29**(4), pp. 1328–1331.